PTEP

Prog. Theor. Exp. Phys. **2018**, 033B03 (21 pages)
DOI: 10.1093/ptep/pty018

125 GeV Higgs boson mass from 5D gauge-Higgs unification

Jason Carson* and Nobuchika Okada*

Department of Physics and Astronomy, University of Alabama, Tuscaloosa, AL 35487, USA
*E-mail: jccarson1@crimson.ua.edu, okadan@ua.edu

Received September 12, 2017; Revised January 30, 2018; Accepted February 4, 2018; Published March 16, 2018

In the context of a simple gauge-Higgs unification (GHU) scenario based on the gauge group $SU(3)\times U(1)'$ in a 5D flat space-time, we investigate the possibility of reproducing the observed Higgs boson mass of around 125 GeV. We introduce bulk fermion multiplets with a bulk mass and a (half-)periodic boundary condition. In our analysis, we adopt a low-energy effective theoretical approach of the GHU scenario, where the running Higgs quartic coupling is required to vanish at the compactification scale. Under this "gauge-Higgs condition," we investigate the renormalization group evolution of the Higgs quartic coupling and find a relation between the bulk mass and the compactification scale so as to reproduce the 125 GeV Higgs boson mass. Through quantum corrections at the one-loop level, the bulk fermions contribute to the Higgs boson production and decay processes and deviate the Higgs boson signal strengths at the Large Hadron Collider experiments from the Standard Model (SM) predictions. Employing the current experimental data that show that the Higgs boson signal strengths for a variety of Higgs decay modes are consistent with the SM predictions, we obtain lower mass bounds on the lightest mode of the bulk fermions to be around 1 TeV.

Subject Index B32, B33, B40

1. Introduction

The discovery of the Standard Model (SM) Higgs boson by the ATLAS [1] and CMS [2] Collaborations at the Large Hadron Collider (LHC) is a milestone in the history of particle physics, and experimental confirmation of the SM Higgs boson properties has just begun. A combined analysis by the ATLAS and CMS Collaborations [3] has determined the Higgs boson mass very precisely as $m_{\rm H} = 125.09 \pm 0.21({\rm stat.}) \pm 0.11({\rm syst.})$ GeV. It has also been shown by combined ATLAS and CMS measurements [4] that the Higgs boson production and decay rates are consistent with the SM predictions. Although the current LHC data include fewer indications for the direct productions of new particles, the Higgs boson can be a portal to reveal new physics beyond the SM through more precise measurements of the Higgs boson properties and their possible deviations from the SM predictions.

The observed Higgs boson mass of around 125 GeV indicates that the electroweak vacuum is unstable [5], since the running SM Higgs quartic coupling becomes negative at the energy around 10^{10} GeV, for the top quark pole mass $M_t = 173.34 \pm 0.76$ from the combined measurements by the Tevatron and the LHC experiments [6].[1] This electroweak vacuum instability may not be a problem, since the lifetime of the electroweak vacuum is estimated to be much longer than the age of the

[1] The stability of the SM Higgs potential is very sensitive to the input value of the top quark pole mass, and we need more precise measurements for it (see, e.g., Ref. [7]).

Funded by SCOAP[3]

universe (meta-stability bound) [8]. However, there are a few discussions that motivate us to take the instability problem seriously: the stability of the Minkowski vacuum has been suggested in terms of consistent quantum field theory [9], and it is unclear if the discussion of the meltability is quantum theoretically consistent or not (see also Refs. [10,11]). Another discussion is based on an inflationary universe. If the Higgs potential has a true anti-de Sitter minimum far away from the electroweak minimum, vacuum fluctuations of the Higgs field in de Sitter space during inflation can push the Higgs field to the unwanted anti-de Sitter vacuum [12,13]. Thus, the electroweak vacuum instability might be a serious problem in particle physics and cosmology. If this is the case, we need to extend the SM to avoid the running Higgs quartic coupling from turning negative at high energy. For example, we may introduce new physics provided by type II [14–17] and type III [18] seesaw mechanisms, which are often invoked in understanding the solar and atmospheric neutrino oscillations, where the running Higgs quartic coupling remains positive in the presence of new particles [19–22].

In this paper, we consider a novel interpretation for the electroweak vacuum instability problem in terms of the gauge-Higgs unification (GHU) scenario [23–28], which is one of the interesting new physics models beyond the SM. In the GHU scenario, the SM Higgs doublet is identified as an extra spacial component of the gauge field in higher-dimensional theory, and the higher-dimensional gauge invariance forbids the quadratic divergence in the self-energy corrections of the Higgs doublet in the SM [29]. As a result, the gauge hierarchy problem can be solved. In this paper, we focus on a simple GHU scenario in the flat 5D space-time and assume that the SM is realized as a low-energy effective theory of the scenario. It has been pointed out [30,31] that in this case the running SM Higgs quartic coupling ($\lambda(\mu)$) must satisfy a special boundary condition (gauge-Higgs condition), namely, $\lambda(M_{\rm KK}) = 0$, where $M_{\rm KK}$ is the compactification scale of the fifth dimension (Kaluza–Klein mass). This condition was derived in Refs. [30,31] as a renormalization condition for the effective Higgs quartic coupling by using an explicit formula of the effective Higgs potential calculated in a simple GHU model. Since the SM Higgs doublet field is provided as the fifth component of the 5D gauge field, there is no Higgs potential at tree level in the GHU scenario. The Higgs potential is radiatively generated at low energies with the breaking of the original gauge symmetry down to the SM gauge group by a certain boundary condition under a fifth-dimensional coordinate transformation. Therefore, in the effective theoretical point of view, we expect that once the original gauge symmetry gets restored at some high energy, the Higgs potential must vanish. This is nothing but the gauge-Higgs condition. Note that the gauge-Higgs condition leads to a new interpretation for the electroweak vacuum instability problem in the SM; i.e., the energy at which $\lambda(\mu) = 0$ is nothing but the compactification scale and the 5D GHU scenario takes place there. there

The gauge-Higgs condition is a powerful tool to calculate the Higgs boson mass irrespective of GHU model details. The Higgs boson mass is easily obtained by solving the renormalization group (RG) equation of the Higgs quartic coupling by imposing the gauge-Higgs condition at a given compactification scale, when the particle contents and the mass spectrum of the low-energy effective theory are defined below the compactification scale. Before the discovery of the SM Higgs boson, the gauge-Higgs condition was utilized to predict the SM Higgs boson mass as a function of the compactification scale, assuming the SM particle contents only [32,33]. After the Higgs boson discovery, the 125 GeV Higgs boson mass indicates that the compactification scale lies around 10^{10} GeV [22,34]. Unfortunately, such a compactification scale is too high to be accessible to any ongoing and planned experiments.

Since the Higgs self-energy induced through the Kaluza–Klein (KK) modes of the SM particles (plus some extra matter in the bulk) is proportional to $M_{\rm KK}^2$, a compactification scale around

the TeV level is desired to solve the gauge hierarchy problem. With only the SM particle contents, the GHU scenario with the TeV compactification scale predicts the Higgs boson mass to be too small, $m_{\rm H} < 100$ GeV. In order to realize the 125 GeV mass, we need to introduce extra fermions in the bulk. In other words, the observed Higgs boson mass implies the existence of exotic fermions in the context of the GHU scenario. In a simple GHU model based on the SU(3)×U(1)′ gauge group, the Higgs boson mass was calculated in the presence of some bulk fermion multiplets such as **10** and **15** representations under the SU(3) [35,36]. It has been shown that the 125 GeV Higgs boson mass can be realized for the TeV compactification scale. The contributions of the bulk fermions to the Higgs boson production and decay processes have also been investigated in Refs. [35,36], and lower bounds on the exotic fermion masses have been obtained from the current LHC data.

The purpose of the present paper is to perform a detailed analysis of the GHU model in Refs. [35,36] and obtain a more accurate bulk fermion mass spectrum to reproduce the 125 GeV Higgs boson mass. In Refs. [35,36], the Higgs boson mass is calculated by solving the RG equation of the Higgs quartic coupling at the leading-log approximation, and no runnings of the gauge couplings and Yukawa couplings have been taken into account. Although this analysis would be good enough to estimate the order of the exotic fermion masses, the resultant mass spectrum is not sufficiently accurate to discuss the experimental search for exotic fermions, since the running gauge and Yukawa couplings are expected to change a lot in the presence of such higher-order representation fermions. In this paper, we will find that our resultant bulk fermion masses to reproduce the 125 GeV Higgs boson mass are quite different from those previously obtained by the rough estimates.

The plan of this paper is as follows. In the next section, we introduce a simple GHU model based on the gauge group SU(3)×U(1)′ [37,38] in a 5D flat space-time with an orbifold S^1/Z_2 compactification to the fifth spacial dimension. As an example, we introduce bulk fermions in the representations of **6** and **10** under the bulk SU(3) gauge group, for which a (half-)periodic boundary condition is imposed. In this context, we evaluate the Higgs boson mass by solving the RG equations with the gauge-Higgs condition and identify the model parameter region to reproduce the observed Higgs boson mass of 125 GeV. In Sect. 3, we study the effects of the bulk fermions on the Higgs boson production and decay processes at the LHC, and derive a lower mass bound on the lightest bulk fermion from the current LHC data. Section 4 is devoted to our conclusions.

2. Higgs boson mass with the gauge-Higgs condition

Let us consider a simple GHU model based on the gauge group SU(3)×U(1)′ in a 5D flat space-time with an orbifolding of the fifth dimension on S^1/Z_2 with a radius R_c of S^1. The extra U(1)′ symmetry works to yield the correct weak mixing angle, and the SM U(1)$_Y$ gauge boson is given by a linear combination between the gauge bosons of the U(1)′ and the U(1) subgroups in SU(3) [37]. One may think that the U(1)$_X$ gauge boson that is orthogonal to the hypercharge U(1)$_Y$ also has a zero mode. However, the U(1)$_X$ symmetry is anomalous in general and broken at the cutoff scale and hence the U(1)$_X$ gauge boson has a mass of the order of the cutoff scale [37]. As a result, zero-mode vector bosons in the model are only the SM gauge fields. In this paper, we employ the effective theoretical approach developed in Refs. [30,31] and evaluate the Higgs boson mass with the gauge-Higgs condition. In this way, we do not discuss how to provide a complete set of bulk fermions whose zero modes correspond to the SM fermions. Among lots of possibilities, we may refer to the proposal in Ref. [38], where the SM fermions are provided with certain SU(3) representations

with a suitable U(1)′ charge to yield the correct hypercharges. In evaluating the Higgs boson mass, what we need is to define the particle contents for particles lighter than the compactification scale.

The boundary conditions should be suitably assigned to reproduce the SM fields as the zero modes. While a periodic boundary condition corresponding to S^1 is taken for all of the bulk SM fields, the Z_2 parity is assigned for gauge fields and fermions in the representation $\mathcal{R}$ by using the parity matrix $P = \mathrm{diag}(-,-,+)$ as

$$A_\mu(-y) = P^\dagger A_\mu(y)P, \quad A_y(-y) = -P^\dagger A_y(y)P, \quad \psi(-y) = \mathcal{R}(P)\psi(y), \tag{1}$$

where the subscripts μ (y) denote the fourth- (fifth-)dimensional component. With this choice of parities, the SU(3) gauge symmetry is explicitly broken to SU(2)×U(1). The hypercharge U(1)$_Y$ is realized as a linear combination of U(1) and U(1)′ in this setup.

With the above parity assignment, off-diagonal blocks in A_y have zero modes, which is identified as the SM Higgs doublet (H) such as

$$A_y^{(0)} = \frac{1}{\sqrt{2}} \begin{pmatrix} 0 & H \\ H^\dagger & 0 \end{pmatrix}. \tag{2}$$

The KK modes of A_y are eaten by KK modes of the SM gauge bosons and enjoy their longitudinal degrees of freedom just like the usual Higgs mechanism.

The parity assignment also provides the SM fermions as massless modes, but in general the massless modes include exotic fermions. In order to make such exotic fermions massive, we may introduce brane-localized fermions with conjugate SU(2)×U(1)$_Y$ charges and an opposite chirality to the exotic fermions and then write mass terms among the exotic fermions on the orbifold fixed points. In the GHU scenario, the Yukawa interaction is unified with the electroweak gauge interaction, so that the SM fermions naturally have the mass of the order of the W-boson mass after electroweak symmetry breaking. This feature is good only for the top quark, while most of the SM fermions are much lighter than the weak boson. To realize light SM fermion masses, one may introduce Z_2-parity odd bulk mass terms for the bulk SM fermions. In the presence of the parity-odd bulk mass, zero-mode fermion wave functions with opposite chirality are localized towards the opposite orbifold fixed points and, as a result, their effective 4D Yukawa coupling is exponentially suppressed by the overlap integral of the wave functions. In this way, we assume that all exotic fermion zero modes become very heavy and realistic SM fermion mass matrices are achieved by adjusting the bulk mass parameters. For more details towards constructing a realistic GHU scenario, see, e.g., Refs. [37,38].

Let us now investigate the way to reproduce the Higgs boson mass of around 125 GeV in this 5D GHU model. It is a highly non-trivial task to propose a realistic GHU scenario and calculate the Higgs boson mass in the context. However, in our effective theory approach, the Higgs boson mass is easily calculated from the RG evolution of the Higgs quartic coupling with the gauge-Higgs condition at the compactification scale, assuming that the electroweak symmetry breaking is correctly achieved. In order to reproduce the 125 GeV Higgs boson mass for $M_{\rm KK} \ll 10^{10}$ GeV, we need to introduce a new fermion in the bulk. In this paper, we introduce color-singlet/triplet **6** and **10**-plet bulk fermions of the bulk SU(3) gauge symmetry with U(1)′ charge Q as an example. We impose a (half-)periodic boundary condition on the bulk fermions, $\psi(y+2\pi R_c) = \psi(y)$ ($\psi(y+2\pi R_c) = -\psi(y)$). To avoid massless states in the periodic bulk fermions, we introduce N_f pairs of the bulk fermion multiplets

with opposite parities and a Z_2-parity even bulk mass term between each pair of bulk fermions. In the same way, we introduce $N_f^{\rm HP}$ pairs of half-periodic fermions with the Z_2-parity even bulk mass term, when we consider half-periodic bulk fermions.[2]

We begin with the **6**-plet of the bulk SU(3) gauge symmetry, which is decomposed into the representations under the SU(2)×U(1) subgroup as

$$\mathbf{6} = \mathbf{1}_{-2/3} \oplus \mathbf{2}_{-1/6} \oplus \mathbf{3}_{1/3}, \tag{3}$$

where the numbers in the subscripts denote the U(1) charges. For these multiplets, the bulk SU(3) gauge interaction leads to a Yukawa interaction of the form

$$\mathcal{L} \supset -Y_S \overline{D} H S - Y_D \overline{D} T H^\dagger, \tag{4}$$

where S, D, and T stand for the singlet, doublet, and triplet fields in the decomposition of Eq. (3), and Y_S and Y_D are Yukawa couplings. Because of the unification of the gauge and Yukawa interactions, $Y_S = Y_D = -ig_2$ at the compactification scale, where g_2 is the SM SU(2) gauge coupling. In solving RG equations, this condition is also imposed as the boundary condition at the compactification scale. After electroweak symmetry breaking the KK mass spectrum is found as follows:

$$\begin{aligned}
\left(m^{(\pm)}_{n,-2/3}\right)^2 &= (m_n \pm 2m_W)^2 + M^2,\ \ m_n^2 + M^2, \\
\left(m^{(\pm)}_{n,+1/3}\right)^2 &= (m_n \pm m_W)^2 + M^2, \\
\left(m^{(\pm)}_{n,+4/3}\right)^2 &= m_n^2 + M^2,
\end{aligned} \tag{5}$$

where the numbers in the subscripts denote the "electric charges"[3] of the corresponding KK mode fermions, $m_n = nM_{\rm KK}$ with $n = 0, 1, 2, \ldots$, $M_{\rm KK} \equiv 1/R_c$, $m_W = g_2 v/2$ with $v = 246$ GeV, and M is a bulk mass. For simplicity, we use a common bulk mass M for the N_f pairs. When a half-periodic boundary condition is imposed on the bulk fermion, the KK mass spectra are obtained by replacing n with $n + 1/2$.

In the same way, we decompose the **10**-plet as

$$\mathbf{10} = \mathbf{1}_{-1} \oplus \mathbf{2}_{-1/2} \oplus \mathbf{3}_0 \oplus \mathbf{4}_{1/2}. \tag{6}$$

For these SM multiplets, the bulk SU(3) gauge interaction leads to a Yukawa interaction of the form

$$\mathcal{L} \supset -Y_S \overline{D} H S - Y_D \overline{D} T H^\dagger - Y_T \overline{F} T H, \tag{7}$$

where S, D, T, and F stand for the singlet, doublet, triplet, and quartet fields in the decomposition of Eq. (6), and Y_S, Y_D, and Y_T are Yukawa couplings. Because of the unification of the gauge and Yukawa interactions, $Y_S = Y_T = -i\sqrt{3/2}\ g_2$ and $Y_D = -i\sqrt{2}\ g_2$ at the compactification scale.

[2] Since no massless mode exists for the half-periodic bulk fermions, the bulk mass term is unnecessary for them. However, the bulk mass parameter along with the other free parameter R_c simplifies our analysis to reproduce the 125 GeV Higgs boson mass. The case with no bulk mass corresponds to $m_0 = M_{\rm KK}/2$ (for notations, see below Eq. (5)). In this case, we cannot reproduce the 125 GeV Higgs boson mass, as we can see from Fig. 5.

[3] Here "electric charges" means the electric charges of SU(2)×U(1)⊂SU(3). The true electric charge of each KK mode is given by the sum of the "electric charge" and the U(1)′ charge Q.

These conditions are imposed as the boundary condition at the compactification scale in our RG analysis. The KK mass spectrum after the electroweak symmetry breaking is found as

$$\begin{aligned}
\left(m^{(\pm)}_{n,-1}\right)^2 &= (m_n \pm 3m_W)^2 + M^2, \quad (m_n \pm m_W)^2 + M^2, \\
\left(m^{(\pm)}_{n,0}\right)^2 &= (m_n \pm 2m_W)^2 + M^2, \quad m_n^2 + M^2, \\
\left(m^{(\pm)}_{n,+1}\right)^2 &= (m_n \pm m_W)^2 + M^2, \\
\left(m^{(\pm)}_{n,+2}\right)^2 &= m_n^2 + M^2.
\end{aligned} \tag{8}$$

Although the U(1)$'$ charge Q is a free parameter of the model, we have phenomenologically favored values for it from the following discussion. As discussed in Ref. [39] (see also Refs. [40–43]), the lightest KK mode of a half-periodic bulk fermion, independently of the background metric, is stable in the effective 4D theory due to an accidental Z_2 discrete symmetry. If the half-periodic bulk fermion is color singlet, it is a good candidate for the cosmological dark matter. Even for the periodic bulk fermion, we are allowed to introduce an odd parity while all the SM particles are even under the parity, in order to ensure the stability of the lightest KK mode. Thus, it is reasonable to assign the U(1)$'$ charge Q to make the lightest KK mode electrically neutral. Since the electric charge is given by the sum of the charge of the U(1) subgroup in the bulk SU(3) and Q, we may choose $Q = 2/3$ ($Q = 1$) for a color-singlet **6**-plet (**10**-plet) bulk fermion. However, a colored stable particle is cosmologically disfavored. For a color-triplet bulk fermion, we may introduce mixing between the lightest colored KK fermion and an SM quark on the brane, so that the lightest KK fermion can decay to the SM quarks. There are two choices for the U(1)$'$ charge to make the electric charge of the lightest KK mode $-1/3$ or $2/3$ for realizing mixing with either SM down-type quarks or up-type quarks. For the **6**-plet case, we may choose $Q = 1/3$ or $4/3$, and $Q = 2/3$ or $5/3$ for the **10**-plet case.

Let us now analyze the RG equations. In our analysis, we neglect the KK mode mass splitting by electroweak symmetry breaking and set the lightest fermion mass as $m_0 = M$. When we impose a half-periodic boundary condition for the bulk fermions,

$$m_0 = \frac{1}{2} M_{\rm KK} \sqrt{1 + 4c_B^2} \tag{9}$$

where $c_B \equiv M/M_{\rm KK}$. For the renormalization scale $\mu < m_0$, the bulk fermions are decoupled, and we employ the SM RG equations at the two-loop level [5]. For the three SM gauge couplings g_i ($i = 1, 2, 3$), we have

$$\frac{dg_i}{d\ln\mu} = \frac{b_i}{16\pi^2} g_i^3 + \frac{g_i^3}{(16\pi^2)^2} \left(\sum_{j=1}^{3} B_{ij} g_j^2 - C_i y_t^2 \right), \tag{10}$$

where the first and second terms on the right-hand side are the beta functions at the one-loop and two-loop levels, respectively, with the coefficients

$$b_i = \left(\frac{41}{10}, -\frac{19}{6}, -7 \right), B_{ij} = \begin{pmatrix} \frac{199}{50} & \frac{27}{10} & \frac{44}{5} \\ \frac{9}{10} & \frac{35}{6} & 12 \\ \frac{11}{10} & \frac{9}{2} & -26 \end{pmatrix}, \; C_i = \left(\frac{17}{10}, \frac{3}{2}, 2 \right). \tag{11}$$

For contributions from the SM Yukawa coupling to the beta function at the two-loop level, we have considered only the top Yukawa coupling (y_t). The RG equation for the top Yukawa coupling is given by

$$\frac{dy_t}{d\ln\mu} = y_t\left(\frac{1}{16\pi^2}\beta_t^{(1)} + \frac{1}{(16\pi^2)^2}\beta_t^{(2)}\right), \tag{12}$$

where the one-loop contribution is

$$\beta_t^{(1)} = \frac{9}{2}y_t^2 - \left(\frac{17}{20}g_1^2 + \frac{9}{4}g_2^2 + 8g_3^2\right), \tag{13}$$

while the two-loop contribution is given by

$$\begin{aligned}\beta_t^{(2)} = &-12y_t^4 + \left(\frac{393}{80}g_1^2 + \frac{225}{16}g_2^2 + 36g_3^2\right)y_t^2 \\ &+ \frac{1187}{600}g_1^4 - \frac{9}{20}g_1^2g_2^2 + \frac{19}{15}g_1^2g_3^2 - \frac{23}{4}g_2^4 + 9g_2^2g_3^2 - 108g_3^4 \\ &+ \frac{3}{2}\lambda^2 - 6\lambda y_t^2.\end{aligned} \tag{14}$$

The RG equation for the quartic Higgs coupling is given by

$$\frac{d\lambda}{d\ln\mu} = \frac{1}{16\pi^2}\beta_\lambda^{(1)} + \frac{1}{(16\pi^2)^2}\beta_\lambda^{(2)}, \tag{15}$$

with the one-loop beta function

$$\beta_\lambda^{(1)} = 12\lambda^2 - \left(\frac{9}{5}g_1^2 + 9g_2^2\right)\lambda + \frac{9}{4}\left(\frac{3}{25}g_1^4 + \frac{2}{5}g_1^2g_2^2 + g_2^4\right) + 12y_t^2\lambda - 12y_t^4 \tag{16}$$

and the two-loop beta function

$$\begin{aligned}\beta_\lambda^{(2)} = &-78\lambda^3 + 18\left(\frac{3}{5}g_1^2 + 3g_2^2\right)\lambda^2 - \left(\frac{73}{8}g_2^4 - \frac{117}{20}g_1^2g_2^2 - \frac{1887}{200}g_1^4\right)\lambda - 3\lambda y_t^4 \\ &+ \frac{305}{8}g_2^6 - \frac{289}{40}g_1^2g_2^4 - \frac{1677}{200}g_1^4g_2^2 - \frac{3411}{1000}g_1^6 - 64g_3^2y_t^4 - \frac{16}{5}g_1^2y_t^4 - \frac{9}{2}g_2^4y_t^2 \\ &+ 10\lambda\left(\frac{17}{20}g_1^2 + \frac{9}{4}g_2^2 + 8g_3^2\right)y_t^2 - \frac{3}{5}g_1^2\left(\frac{57}{10}g_1^2 - 21g_2^2\right)y_t^2 - 72\lambda^2y_t^2 + 60y_t^6.\end{aligned} \tag{17}$$

In solving the RG equations, we use the boundary conditions at the top quark pole mass (M_t) given in Ref. [5]:

$$\begin{aligned}g_1(M_t) &= \sqrt{\frac{5}{3}}\left(0.357\,61 + 0.000\,11(M_t - 173.10) - 0.000\,21\left(\frac{m_W - 80.384}{0.014}\right)\right), \\ g_2(M_t) &= 0.648\,22 + 0.000\,04(M_t - 173.10) + 0.000\,11\left(\frac{m_W - 80.384}{0.014}\right), \\ g_3(M_t) &= 1.1666 + 0.003\,14\left(\frac{\alpha_s - 0.1184}{0.0007}\right), \\ y_t(M_t) &= 0.935\,58 + 0.0055(Mt - 173.10) - 0.000\,42\left(\frac{\alpha_s - 0.1184}{0.0007}\right) - 0.000\,42\left(\frac{m_W - 80.384}{0.014}\right), \\ \lambda(M_t) &= 2(0.127\,11 + 0.002\,06(m_{\rm H} - 125.66) - 0.000\,04(M_t - 173.10)).\end{aligned} \tag{18}$$

We employ $m_W = 80.384$ (in GeV), $\alpha_s = 0.1184$, $M_t = 173.34$ (in GeV) from the combined measurements by the Tevatron and LHC experiments [6], and $m_{\rm H} = 125.09$ (in GeV) from the combined analysis by ATLAS and CMS [3].

For the renormalization scale $\mu \geq m_0$, the SM RG equations are modified in the presence of the bulk fermions. In this paper, we take only one-loop corrections from the bulk fermions into account. For the case with N_f pairs of **6**-plet periodic fermions (we identify N_f as $N_f = 2N_f^{\rm HP}$ for the case with $N_f^{\rm HP}$ pairs of half-periodic fermions), the beta functions of the SU(2) and U(1)$_Y$ gauge couplings receive new contributions as

$$\Delta b_1 = N_f N_c \left(\frac{2}{3} + \frac{24}{5}Q^2\right), \quad \Delta b_2 = \frac{10}{3}N_f N_c, \quad \Delta b_3 = 4N_f \left(\frac{N_c - 1}{2}\right), \tag{19}$$

where $N_c = 1$ ($N_c = 3$) when the **6**-plet bulk fermions are color singlet (triplet). The beta functions of the top Yukawa and Higgs quartic couplings are modified as

$$\begin{aligned}
&\beta_t^{(1)} \to \beta_t^{(1)} + y_t N_f N_c \left(2|Y_S|^2 + 3|Y_D|^2\right), \\
&\beta_\lambda^{(1)} \to \beta_\lambda^{(1)} + N_f N_c \left[\lambda\left(8|Y_S|^2 + 12|Y_D|^2\right) - \left(8|Y_S|^4 + 10|Y_D|^4 + 16|Y_S|^2|Y_D|^2\right)\right],
\end{aligned} \tag{20}$$

where the Yukawa couplings obey the following RG equations:

$$\begin{aligned}
16\pi^2 \frac{dY_S}{d\ln\mu} = Y_S \Bigg[& 3y_t^2 - \left(\frac{9}{20}g_1^2 + \frac{9}{4}g_2^2\right) + N_f \left(\frac{4N_c + 3}{2}|Y_S|^2 + \frac{12N_c + 7}{4}|Y_D|^2\right) \\
& - (N_c^2 - 1)g_3^2 - \frac{18}{5}\left(\frac{2}{3} - Q\right)\left(\frac{1}{6} - Q\right)g_1^2 \Bigg], \\
16\pi^2 \frac{dY_D}{d\ln\mu} = Y_D \Bigg[& 3y_t^2 - \left(\frac{9}{20}g_1^2 + \frac{9}{4}g_2^2\right) + N_f \left(\frac{4N_c + 5}{2}|Y_S|^2 + \frac{12N_c + 5}{4}|Y_D|^2\right) \\
& - (N_c^2 - 1)g_3^2 - 6g_2^2 - \frac{18}{5}\left(\frac{1}{6} - Q\right)\left(\frac{1}{3} - Q\right)g_1^2 \Bigg].
\end{aligned} \tag{21}$$

In our RG analysis, we numerically solve the SM RG equations from M_t to m_0, at which the solutions connect with the solutions of the RG equations with the bulk fermions. For a fixed m_0 value, we arrange the input values for $Y_S(m_0)$ and $Y_D(m_0)$ so as to find the numerical solutions that satisfy the gauge-Higgs condition and the unification condition between the gauge and Yukawa couplings at the compactification scale:

$$\lambda(M_{\rm KK}) = 0, \quad Y_S(M_{\rm KK}) = Y_D(M_{\rm KK}) = -ig_2(M_{\rm KK}). \tag{22}$$

The running Higgs quartic coupling to reproduce the Higgs boson pole mass of $m_{\rm H} = 125.09$ GeV is shown in Fig. 1. The solid line denotes the running quartic coupling in the SM, while the dashed (dotted) line corresponds to the result for the case with an $N_f = 2$ ($N_f = 1$) pair of **6**-plet color-singlet (-triplet) bulk fermions with U(1)$'$ charge $Q = 2/3$ ($Q = 4/3$). For the dashed (dotted) line, we find $M_{\rm KK} = 12.7$ (5.65) TeV for $m_0 = 1.5$ TeV, at which the gauge-Higgs condition is satisfied. When we trace the dashed and dotted lines from M_t to higher energies we see that the running of the Higgs quartic coupling is drastically altered from the SM one (solid line) due to the contributions from the bulk fermions with $m_0 = 1.5$ TeV. Since the beta function of the Higgs quartic coupling becomes more negative in the presence of the bulk fermions (see Eq. (20)), the running Higgs quartic coupling reaches the compactification scale far below 10^{10} GeV. We also show in Fig. 2

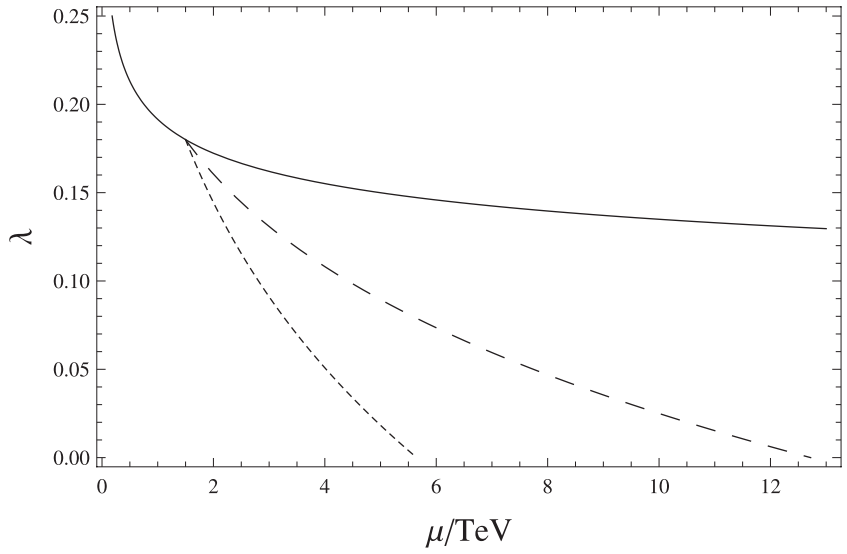

Fig. 1. The RG evolutions of the Higgs quartic coupling, which can reproduce the Higgs boson pole mass of $m_{\rm H} = 125.09$ GeV. The solid line denotes the running Higgs quartic coupling in the SM. The dashed and dotted lines correspond, respectively, to the **6**-plets for $N_f = 2, N_c = 1, Q = 2/3$, and $(M_{\rm KK}, m_0) = (12.7, 1.5)$ TeV and the **6**-plet for $N_f = 1, N_c = 3, Q = 4/3$, and $(M_{\rm KK}, m_0) = (5.65, 1.5)$ TeV.

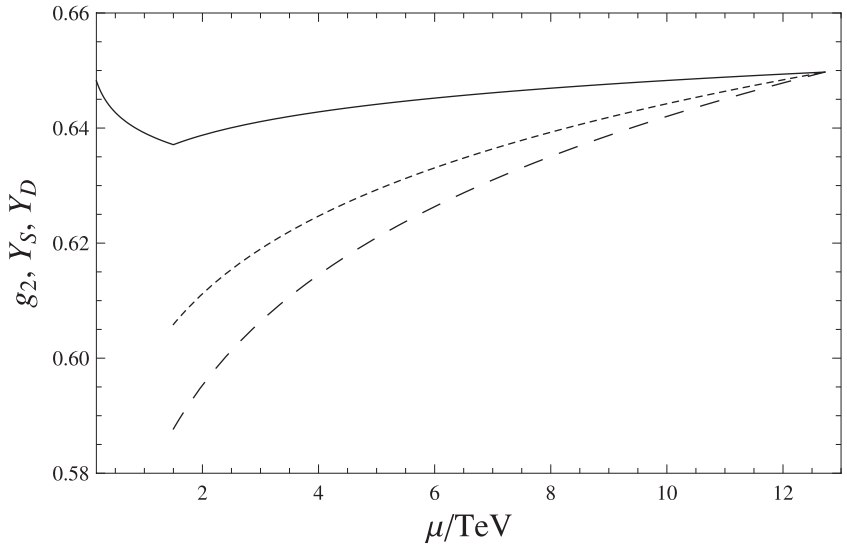

Fig. 2. The RG evolutions of the SM SU(2) gauge coupling (solid line) and Yukawa couplings, $|Y_S|$ (dashed line) and $|Y_D|$ (dotted line), for the case with an $N_f = 2$ pair of **6**-plet color-singlet bulk fermions with $Q = 2/3$. We can see that the boundary condition from the unification among the gauge and Yukawa couplings, $|Y_S| = |Y_D| = g_2$, is satisfied at $M_{\rm KK} = 12.7$ TeV.

the RG evolutions of the SM SU(2) gauge coupling (solid line) and Yukawa couplings $|Y_S|$ (dashed line) and $|Y_D|$ (dotted line) for the case with an $N_f = 2$ pair of **6**-plet color-singlet bulk fermions with $Q = 2/3$, corresponding to the dashed line in Fig. 1. We can see that the boundary condition from the unification between the gauge and Yukawa couplings, $|Y_S| = |Y_D| = g_2$, is satisfied at $M_{\rm KK} = 12.7$ TeV. It is interesting to compare Fig. 1 with Fig. 4 in Ref. [35]. We can see that the RG evolutions shown in these figures are quite different. This difference is due to the RG effects of the gauge and Yukawa couplings that are taken into account in our analysis. Hence, our resultant bulk

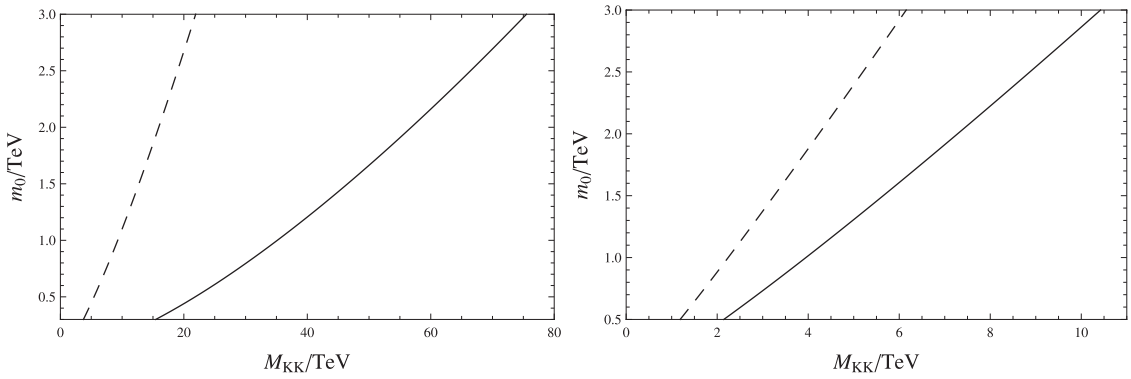

Fig. 3. The relation between M_{KK} and m_0 to reproduce the Higgs boson pole mass of $m_H = 125.09$ GeV. The left panel shows the results for the color-singlet **6**-plet bulk fermions with $N_f = 1$ (solid line) and $N_f = 2$ (dashed line). Here we have taken $Q = 2/3$. The right panel shows the results for the color-triplet **6**-plet bulk fermions with $N_f = 1$ (solid line) and $N_f = 2$ (dashed line). For the color-triplet case, we have taken $Q = 4/3$.

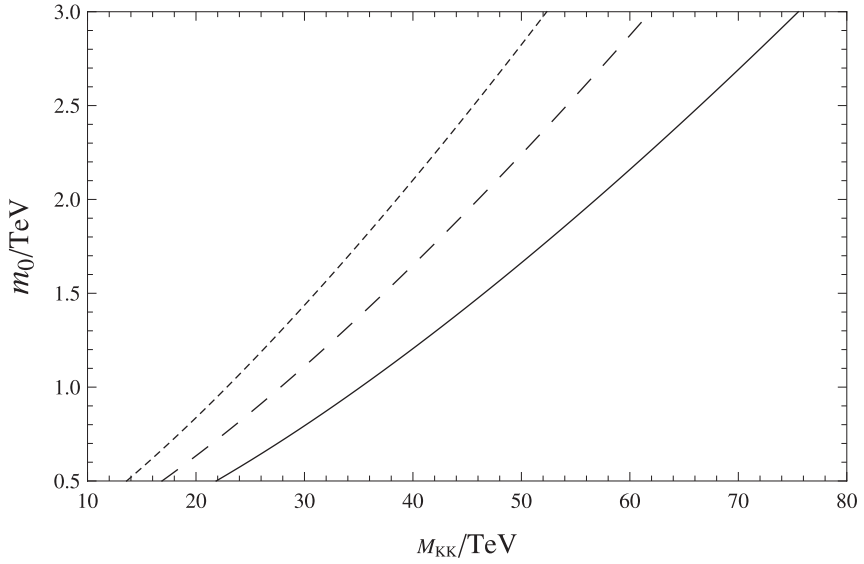

Fig. 4. In the case with the color-singlet **6**-plet bulk fermions ($N_f = 1$), the relation between M_{KK} and m_0 to reproduce the Higgs boson pole mass of $m_H = 125.09$ GeV for various U(1)$'$ charges is shown. The solid, dashed, and dotted lines correspond to the results for $Q = 0$, 2, and -2, respectively.

fermion masses to reproduce the 125 GeV Higgs boson mass are quite different from those obtained in Refs. [35,36], as we have mentioned in Sect. 1.

Once the lightest fermion mass m_0 is fixed, the compactification scale M_{KK} is determined, where the gauge-Higgs condition and the unification condition between the gauge and Yukawa couplings are satisfied. The relation between M_{KK} and m_0 is depicted in Fig. 3. In the left panel we show the relation for the color-singlet **6**-plet bulk fermions with $N_f = 1$ (solid line) and $N_f = 2$ (dashed line). Here we have taken $Q = 2/3$ as an example. The relations for the color-triplet **6**-plet bulk fermions with $N_f = 1$ (solid line) and $N_f = 2$ (dashed line), respectively, are shown in the right panel. For the color-triplet case, we have taken $Q = 4/3$. As the number of bulk fermions increases, the compactification scale for a fixed m_0 decreases.

For the color-singlet **6**-plet bulk fermions with $N_f = 1$, we show in Fig. 4 the relation between M_{KK} and m_0 for various U(1)$'$ charges. The solid, dashed, and dotted lines correspond to the results

for $Q = 0$, 2, and -2, respectively. We find that the compactification scale for a fixed m_0 decreases as $|Q|$ increases.

We perform the same analysis for the case with N_f pairs of the **10**-plet periodic fermions (we identify N_f as $N_f = 2N_f^{\rm HP}$ for the case with $N_f^{\rm HP}$ pairs of half-periodic fermions). For the renormalization scale $\mu \geq m_0$, the beta functions of the SU(2) and U(1)$_Y$ gauge couplings receive new contributions as

$$\Delta b_1 = N_f N_c \left(3 + 12Q^2\right), \quad \Delta b_2 = 10 N_f N_c, \quad \Delta b_3 = \frac{10}{3} N_f \left(\frac{N_c - 1}{2}\right), \tag{23}$$

where $N_c = 1$ ($N_c = 3$) when the **10**-plet bulk fermions are color singlet (triplet). The beta functions of the top Yukawa and Higgs quartic couplings are modified as

$$\begin{aligned}
\beta_t^{(1)} &\to \beta_t^{(1)} + y_t N_f N_c \left(2|Y_S|^2 + 3|Y_D|^2\right), \\
\beta_\lambda^{(1)} &\to \beta_\lambda^{(1)} + N_f N_c \Big[4\lambda \left(2|Y_S|^2 + 3|Y_D|^2 + 4|Y_T|^2\right) \\
&\quad - \left(8|Y_S|^4 + 10|Y_D|^4 + \frac{112}{9}|Y_T|^4 + 16|Y_S|^2|Y_D|^2 + \frac{64}{3}|Y_D|^2|Y_T|^2\right)\Big],
\end{aligned} \tag{24}$$

where the Yukawa couplings obey the following RG equations:

$$\begin{aligned}
16\pi^2 \frac{dY_S}{d\ln\mu} &= Y_S \Big[3y_t^2 - \left(\frac{9}{20}g_1^2 + \frac{9}{4}g_2^2\right) + N_f \left(\frac{4N_c + 3}{2}|Y_S|^2 + \frac{12N_c + 15}{4}|Y_D|^2 + 4N_c|Y_T|^2\right) \\
&\quad - (N_c^2 - 1)g_3^2 - \frac{18}{5}(1 - Q)\left(\frac{1}{2} - Q\right)g_1^2\Big], \\
16\pi^2 \frac{dY_D}{d\ln\mu} &= Y_D \Big[3y_t^2 - \left(\frac{9}{20}g_1^2 + \frac{9}{4}g_2^2\right) + N_f \left(\frac{4N_c + 5}{2}|Y_S|^2 + \frac{12N_c + 5}{4}|Y_D|^2 + \frac{12N_c + 10}{3}|Y_T|^2\right) \\
&\quad - (N_c^2 - 1)g_3^2 - 6g_2^2 - \frac{18}{5}\left(Q - \frac{1}{2}\right)Q\, g_1^2\Big], \\
16\pi^2 \frac{dY_T}{d\ln\mu} &= Y_T \Big[3y_t^2 - \left(\frac{9}{20}g_1^2 + \frac{9}{4}g_2^2\right) + N_f \left(2N_c|Y_S|^2 + \frac{6N_c + 5}{2}|Y_D|^2 + \frac{24N_c + 7}{6}|Y_T|^2\right) \\
&\quad - (N_c^2 - 1)g_3^2 - 15g_2^2 - \frac{18}{5}Q\left(Q + \frac{1}{2}\right)g_1^2\Big].
\end{aligned} \tag{25}$$

We numerically solve the SM RG equations from M_t to m_0, at which the solutions connect with the solutions of the RG equations with the **10**-plet bulk fermions. For a fixed m_0 value, we arrange the input values for $Y_S(m_0)$, $Y_D(m_0)$ and $Y_T(m_0)$ so as to find the numerical solutions that satisfy the gauge-Higgs condition and the unification condition between the gauge and Yukawa couplings at the compactification scale:

$$\lambda(M_{\rm KK}) = 0, \quad \sqrt{\frac{2}{3}}Y_S(M_{\rm KK}) = \sqrt{\frac{1}{2}}Y_D(M_{\rm KK}) = \sqrt{\frac{2}{3}}Y_T(M_{\rm KK}) = -ig_2(M_{\rm KK}). \tag{26}$$

In Fig. 5, we show the relation between $M_{\rm KK}$ and m_0. The solid and dashed lines denote the results for the color-singlet **10**-plet bulk fermions with $N_f = 1$ and $N_f = 2$, respectively. Here we have taken $Q = 1$. The dotted and dash-dotted lines represent the results for the color-triplet **10**-plet bulk fermions with $N_f = 1$ and $N_f = 2$, respectively. We have taken $Q = 5/3$ for the color-triplet **10**-plets. Note that along the dash-dotted line the relation of $m_0 \geq M_{\rm KK}/2$ is satisfied, and we can also consider a half-periodic boundary condition for this case with $N_f^{\rm HP} = 1$.

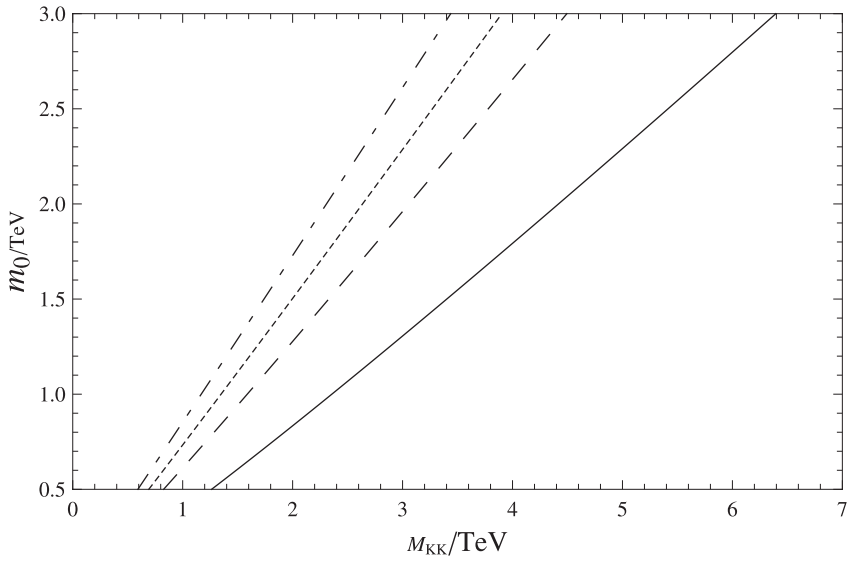

Fig. 5. The relation between $M_{\rm KK}$ and m_0 to reproduce the Higgs boson pole mass of $m_{\rm H} = 125.09$ GeV. The solid and dashed lines denote the results for the color-singlet **10**-plet bulk fermions with $N_f = 1$ and $N_f = 2$, respectively. Here we have taken $Q = 1$. The dotted and dash-dotted lines represent the results for the color-triplet **10**-plet bulk fermions with $N_f = 1$ and $N_f = 2$ ($N_f^{\rm HP} = 1$), respectively. We have taken $Q = 5/3$ for the **10**-plets.

3. Higgs boson production and decay in the GHU model

Through quantum corrections at the one-loop level, the bulk fermions contribute to the Higgs boson production and decay processes and deviate the Higgs boson signal strengths at the LHC experiments from the SM predictions. In this section, we evaluate the contributions from the bulk **6**-plet and **10**-plet fermions to the Higgs boson production and decay processes at the LHC, leading to a lower mass bound for the lightest bulk fermion.

3.1. Bulk fermion contributions to the gluon fusion channel

At the LHC, the Higgs boson is dominantly produced via the gluon fusion process with the following dimension-five operator between the Higgs boson and di-gluon:

$$\mathcal{L}_{\rm eff} = C_{gg} h G^a_{\mu\nu} G^{a\mu\nu}, \tag{27}$$

where h is the SM Higgs boson, and $G^a_{\mu\nu}$ ($a = 1$–8) is the gluon field strength. The SM contribution to C_{gg} is dominated by top quark one-loop corrections. As a good approximation, we express this contribution by using the Higgs low-energy theorem [44],

$$C_{gg}^{\rm SMtop} \simeq \frac{g_3^2}{32\pi^2 v} b_3^t \frac{\partial}{\partial \log v} \log M_t = \frac{\alpha_s}{12\pi v}, \tag{28}$$

where $\alpha_s = g_3^2/(4\pi)$, and $b_3^t = 2/3$ is a top quark contribution to the beta function coefficient of QCD.

In addition to the SM contribution, we take into account the contributions from the top quark KK modes. One might think that the KK mode contributions from the light SM fermions should be taken into account. However, they can be neglected compared to those from the top quark KK modes, since the effective coupling of the Higgs boson to the di-gluon is generated by electroweak

symmetry breaking and hence is proportional to the corresponding SM fermion masses. Thus, we only consider the top quark KK mode contribution. In the GHU scenario, we expect the top quark KK mode spectrum to be

$$m_{n,t}^{(\pm)} = m_n \pm M_t, \tag{29}$$

where $m_n \equiv nM_{\rm KK}$ with an integer $n = 1, 2, 3, \ldots$. Using the Higgs low-energy theorem, we obtain

$$\begin{aligned} C_{gg}^{\rm KKtop} &\simeq \frac{\alpha_s}{12\pi v} \sum_{n=1}^{\infty} \frac{\partial}{\partial \log v} \left[\log(m_n + M_t) + \log(m_n - M_t)\right] \\ &\simeq -\frac{\alpha_s}{6\pi v} \sum_{n=1}^{\infty} \left(\frac{M_t}{m_n}\right)^2 = -\frac{\alpha_s}{12\pi v} \times \frac{\pi^2}{3} \left(\frac{M_t}{M_{\rm KK}}\right)^2, \end{aligned} \tag{30}$$

where we have used an approximation of $M_t^2 \ll m_n^2$, and $\sum_{n=1}^{\infty} 1/n^2 = \pi^2/6$. As pointed out in Ref. [45], the KK mode contribution to the effective Higgs coupling to the di-gluon is destructive to the SM one.

N_f pairs of color-triplet **6**-plet and **10**-plet bulk fermions have the KK mass spectra as shown in Eqs. (5) and (8), respectively. Applying the Higgs low-energy theorem, their contributions to the Higgs–di-gluon coupling are calculated as

$$C_{gg}^{\rm KK6} \simeq F(2m_W) + F(m_W), \tag{31}$$

$$C_{gg}^{\rm KK10} \simeq F(3m_W) + F(2m_W) + 2F(m_W), \tag{32}$$

where the function $F(m_W)$ is given by

$$\begin{aligned} F(m_W) &= 2N_f \frac{\alpha_s}{12\pi v} \sum_{n=-\infty}^{\infty} \frac{\partial}{\partial \log v} \left[\log \sqrt{(m_n + m_W)^2 + M^2}\right] \\ &\simeq 2N_f \frac{\alpha_s}{12\pi v} \left(\frac{m_W}{M_{\rm KK}}\right)^2 \left[\frac{1}{c_B^2 + (m_W/M_{\rm KK})^2} - 2\sum_{n=1}^{\infty} \frac{n^2 - c_B^2}{\left(n^2 + c_B^2\right)^2}\right] \\ &= 2N_f \frac{\alpha_s}{12\pi v} \left(\frac{m_W}{M_{\rm KK}}\right)^2 \left[\frac{1}{c_B^2 + (m_W/M_{\rm KK})^2} - \frac{1 - (\pi c_B/\sinh[\pi c_B])^2}{c_B^2}\right], \end{aligned} \tag{33}$$

for the bulk fermion for which a periodic boundary condition is imposed. Note that $F(m_W)$ is positive since the zero-mode ($n = 0$) contribution dominates over the negative KK mode contributions. When we impose a half-periodic boundary condition, we have [35,36]

$$\begin{aligned} F(m_W) &= 2N_f^{\rm HP} \frac{\alpha_s}{12\pi v} \sum_{n=-\infty}^{\infty} \frac{\partial}{\partial \log v} \left[\log \sqrt{M^2 + (m_{n+\frac{1}{2}} + m_W)^2}\right] \\ &\simeq -2N_f^{\rm HP} \frac{\alpha_s}{6\pi v} \left(\frac{m_W}{M_{\rm KK}}\right)^2 \sum_{n=0}^{\infty} \frac{\left(n + \frac{1}{2}\right)^2 - c_B^2}{\left(\left(n + \frac{1}{2}\right)^2 + c_B^2\right)^2} \\ &= -2N_f^{\rm HP} \frac{\alpha_s}{12\pi v} \left(\frac{m_W}{M_{\rm KK}}\right)^2 \frac{\pi^2}{\cosh^2[\pi c_B]}. \end{aligned} \tag{34}$$

Here, $c_B = M/M_{\rm KK}$, and we have used the approximation $m_W^2 \ll M_{\rm KK}^2$.

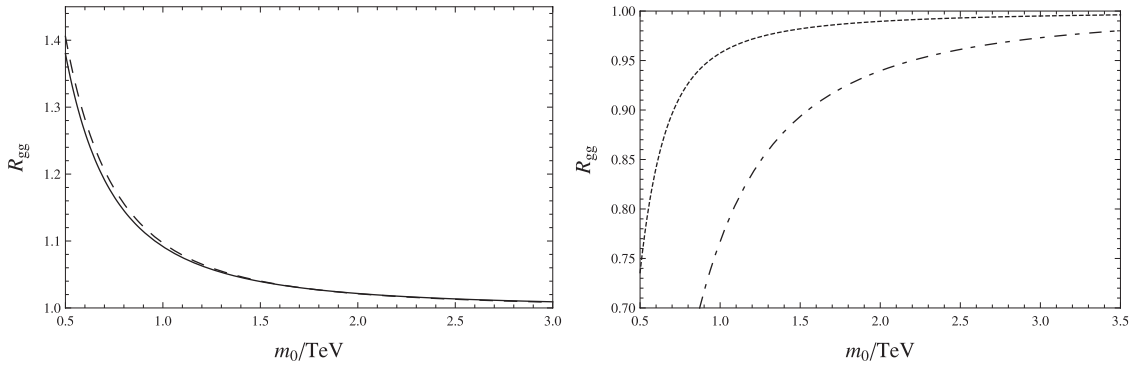

Fig. 6. The ratio of the Higgs production cross section in our model to the SM one as a function of the lightest bulk fermion mass m_0. The left panel shows the results for the **6**-plet case corresponding to the right panel of Fig. 3. The results for the **10**-plet case, corresponding to the dotted and dash-dotted lines in Fig. 5, are depicted in the right panel. Here we have considered the periodic boundary condition for the dotted line in Fig. 5, and the half-periodic boundary condition for the dash-dotted line in Fig. 5. The dotted and dash-dotted lines represent the results for the periodic and half-periodic **10**-plet fermions, respectively.

Now we evaluate the ratio of the Higgs production cross section through the gluon fusion at the LHC to the SM one as

$$R_{gg} \equiv \left(1 + \frac{C_{gg}^{\rm KKtop} + C_{gg}^{\rm KK6/10}}{C_{gg}^{\rm SMtop}}\right)^2 . \tag{35}$$

In the previous section, we have found a relation between $M_{\rm KK}$ and m_0 for the color-triplet bulk fermions to reproduce the Higgs boson pole mass of $m_{\rm H} = 125.09$ GeV (see Figs. 3 and 5). With the relation, we can express the ratio R_{gg} as a function of m_0. Our results are shown in Fig. 6. The left panel shows the ratio in the presence of the color-triplet bulk **6**-plet fermions for which the relation between $M_{\rm KK}$ and m_0 are shown in the right panel of Fig. 3. The solid and dashed lines in the left panel of Fig. 6 correspond to the solid and dashed lines in the right panel of Fig. 3. The right panel of Fig. 6 shows the results for the color-triplet **10**-plet bulk fermions. The relations between $M_{\rm KK}$ and m_0 for the fermions are shown as the dotted and the dash-dotted lines in Fig. 5. Note that the relation along the dash-dotted line satisfies $m_0 \geq M_{\rm KK}/2$, so that we can also apply a half-periodic boundary condition for the **10**-plet fermions with $N_f^{\rm HP} = 1$. Here we have considered the periodic boundary condition for the dotted line in Fig. 5, and the half-periodic boundary condition for the dash-dotted line in Fig. 5. The dotted and dash-dotted lines represent the results for the periodic and half-periodic **10**-plet fermions, respectively.

In the presence of the bulk fermions, the Higgs production cross section in the gluon fusion channel is altered from the SM prediction. This deviation becomes larger as m_0 (or equivalently, $M_{\rm KK}$) is reduced. Since the Higgs boson properties measured by the LHC experiments are found to be consistent with the SM predictions [4], we can find a lower bound for m_0 from the LHC results. Employing the results from a combined analysis by the ATLAS and CMS Collaborations [4], $0.89 \leq R_{gg} \leq 1.19$, we can read off a lower bound of the lightest bulk fermion mass m_0 from Fig. 6. Our results are summarized in Table 1. The lower bounds are found to be at the TeV scale, so that such exotic colored particles can be tested at the LHC Run-2 with $\sqrt{s} = 13$–14 TeV.

Table 1. The lower bound on the lightest bulk fermion masses and the compactification scales from the ATLAS and CMS combined analysis, $0.89 \leq R_{gg} \leq 1.19$, for the cases with the color-triplet **6** or **10**-plet bulk fermion. Here, the initials "BC", "P", and "HP" stand for "boundary condition", "periodic", and "half-periodic", respectively. We have also shown in the last row the lower bound on the compactification scale when only the top quark KK modes are taken into account.

	BC	$N_f^{(\mathrm{HP})}$	Q	m_0 (TeV)	M_{KK} (TeV)
6-plet	P	1	4/3	0.703	2.89
6-plet	P	2	4/3	0.728	1.67
10-plet	P	1	5/3	0.685	0.937
10-plet	HP	1	5/3	1.48	1.71
top quark KK mode					1.32

3.2. Bulk fermion contributions to $h \to \gamma\gamma$

Since the bulk fermions have electric charges, they also contribute to the effective Higgs boson coupling with a di-photon of the dimension-five operator,

$$\mathcal{L}_{\mathrm{eff}} = C_{\gamma\gamma} h F_{\mu\nu} F^{\mu\nu}, \tag{36}$$

where $F_{\mu\nu}$ denotes the photon field strength. In the SM, this effective coupling is induced by the top quark and W-boson loop corrections. In addition to the SM contributions, we have contributions from the KK modes of the top quark, W-boson, and the **6**-plet or **10**-plet bulk fermion.

We begin with the top quark loop contribution. By using the Higgs low-energy theorem, we have

$$C_{\gamma\gamma}^{\mathrm{SMtop}} \simeq \frac{e^2 b_1^t}{32\pi^2 v} \frac{\partial}{\partial \log v} \log m_t = \frac{2\alpha_{em}}{9\pi v}, \tag{37}$$

where $b_1 = (4/3)\times(2/3)^2\times 3 = 4/3$ is a top quark contribution to the QED beta function coefficient, and α_{em} is the fine structure constant. The corresponding KK top quark contribution is given by

$$\begin{aligned} C_{\gamma\gamma}^{\mathrm{KKtop}} &\simeq \frac{e^2 b_1^t}{32\pi^2 v} \sum_{n=1}^{\infty} \frac{\partial}{\partial \log v} \left[\log(m_n + M_t) + \log(m_n - M_t)\right] \\ &\simeq -\frac{2\alpha_{em}}{9\pi v} \times \frac{\pi^2}{3} \left(\frac{M_t}{M_{\mathrm{KK}}}\right)^2. \end{aligned} \tag{38}$$

As with the contribution to the effective Higgs coupling with the di-gluon, the KK top quark contribution is destructive to the top quark contribution.

Applying the Higgs low-energy theorem, the SM W-boson loop contribution is calculated as

$$C_{\gamma\gamma}^{W} \simeq \frac{e^2}{32\pi^2 v} b_1^W \frac{\partial}{\partial \log v} \log m_W = -\frac{7\alpha_{em}}{8\pi v}, \tag{39}$$

where $m_W = g_2 v/2$, and $b_1^W = -7$ is a W-boson contribution to the QED beta function coefficient. Since $4m_W^2/m_h^2 \gg 1$ is not well satisfied, this estimate is rough. In the following numerical analysis, we use the known loop-function for the W-boson loop correction [44].

In our model, the KK mode mass spectrum of the W-boson is given by

$$m_{n,W}^{(\pm)} = m_n \pm m_W, \tag{40}$$

so that the contribution from KK W-boson loop diagrams is found to be

$$C_{\gamma\gamma}^{\rm KKW} = \frac{e^2}{32\pi^2 v} b_1^W \sum_{n=1}^{\infty} \frac{\partial}{\partial \log v} \left[\log(m_n + m_W) + \log(m_n - m_W)\right]$$
$$\simeq \frac{7\alpha_{em}}{8\pi v}\frac{\pi^2}{3}\left(\frac{m_W}{M_{\rm KK}}\right)^2. \tag{41}$$

Note again that the KK W-boson contribution is destructive to the SM W-boson contribution.

Finally, the **6**-plet or **10**-plet loop contributions can be read from the KK mode mass spectrum in Eqs. (5) or (8) and the electric charges of each mode:

$$C_{\gamma\gamma}^{\rm KK6} \simeq \left(Q - \frac{2}{3}\right)^2 \hat{F}(2m_W) + \left(Q + \frac{1}{3}\right)^2 \hat{F}(m_W) \tag{42}$$

$$C_{\gamma\gamma}^{\rm KK10} \simeq (Q-1)^2\hat{F}(3m_W) + (Q-1)^2\hat{F}(m_W) + Q^2\hat{F}(2m_W) + (Q+1)^2\hat{F}(m_W), \tag{43}$$

where Q is a $U(1)'$ charge for the **6** and **10**-plets, and

$$\hat{F}(m_W) \simeq 2N_f N_c \frac{\alpha_{em}}{6\pi v}\left(\frac{m_W}{M_{\rm KK}}\right)^2 \left[\frac{1}{c_B^2 + (m_W/M_{\rm KK})^2} - \frac{1 - (\pi c_B/\sinh[\pi c_B])^2}{c_B^2}\right], \tag{44}$$

for the periodic bulk fermions, while for the half-periodic bulk fermions, we have

$$\hat{F}(m_W) \simeq -2N_f^{\rm HP} N_c \frac{\alpha_{em}}{6\pi v}\left(\frac{m_W}{M_{\rm KK}}\right)^2 \frac{\pi^2}{\cosh^2[\pi c_B]}. \tag{45}$$

Here, we have used the approximation $m_W^2 \ll M_{\rm KK}^2$. Similarly to Eq. (33), $\hat{F}(m_W)$ in Eq. (44) is positive since the zero-mode contribution dominates.

The ratio of the partial decay width of $h \to \gamma\gamma$ in our model to the SM one is given by

$$R_{\gamma\gamma} = \left(1 + \frac{C_{\gamma\gamma}^{\rm KKtop} + C_{\gamma\gamma}^{\rm KKW} + C_{\gamma\gamma}^{\rm KK6/10}}{C_{\gamma\gamma}^{\rm SMtop} + C_{\gamma\gamma}^{W}}\right)^2. \tag{46}$$

If the bulk fermions are color singlet, they have no effect on the Higgs boson production cross section. In this case, the effect of the bulk fermions can be seen in a deviation of the signal strength of the Higgs di-photon decay mode. Since the branching fraction of $h \to \gamma\gamma$ is of the order of 0.1%, the deviation of the signal strength from the SM prediction is evaluated by $R_{\gamma\gamma}$. The relation between m_0 and $M_{\rm KK}$ is determined so as to reproduce $m_{\rm H} = 125.09$ GeV; we evaluate $R_{\gamma\gamma}$ as a function of m_0 for the color-singlet **6**-plet and **10**-plet bulk fermions. Our results are shown in Fig. 7. The left panel shows the results for the **6**-plet case presented in the left panel of Fig. 3. The solid and dashed lines correspond to the same types of lines in the left panel of Fig. 3. The results for the **10**-plet case, which correspond to the solid and dashed lines in Fig. 5, are depicted in the right panel.

To derive a lower bound on m_0, we employ the results of the signal strength from a combined analysis by the ATLAS and CMS Collaborations [4], such as $0.96 \leq \mu^{\gamma\gamma} \leq 1.33$, which is identified as $R_{\gamma\gamma}$ in our case. We then read off a lower bound on the lightest bulk fermion mass m_0 from Fig. 7. Our results are summarized in Table 2.

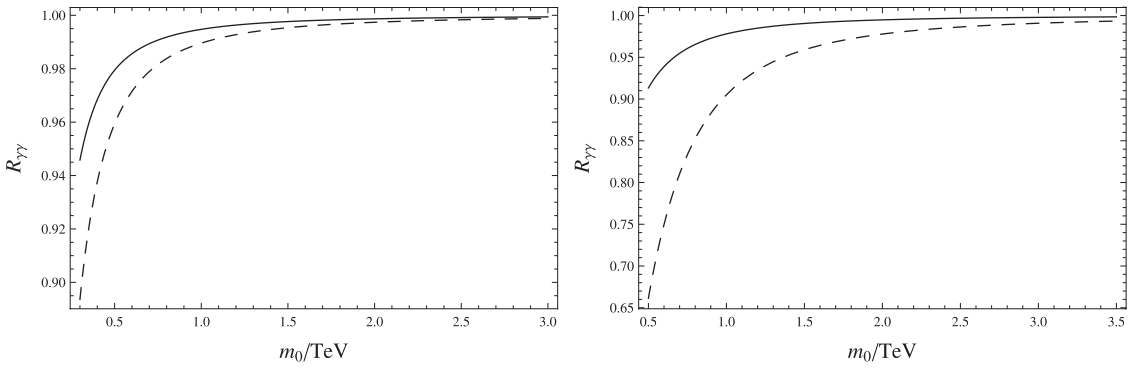

Fig. 7. The signal strength for the Higgs di-photon decay mode in our model as a function of the lightest bulk fermion mass m_0. The left panel shows the results for the **6**-plet case corresponding to the left panel of Fig. 3. The results for the **10**-plet case, which correspond to the solid and dashed lines in Fig. 5, are depicted in the right panel.

Table 2. The lower bound on the lightest bulk fermion masses and the compactification scales from the ATLAS and CMS combined analysis, $0.96 \leq \mu^{\gamma\gamma} \simeq R_{\gamma\gamma} \leq 1.33$, for the cases with the color-singlet **6** and **10**-plet bulk fermions.

	BC	N_f	Q	m_0 (TeV)	$M_{\rm KK}$ (TeV)
6-plet	P	1	2/3	0.353	17.2
6-plet	P	2	2/3	0.504	5.48
10-plet	P	1	1	0.744	1.81
10-plet	P	2	1	1.52	2.35

3.3. Bulk colored fermion contributions to $gg \to h \to \gamma\gamma$

Finally, we calculate the signal strength of the process $gg \to h \to \gamma\gamma$ in our model. The bulk colored fermions contribute to both the effective Higgs coupling to the di-gluon and di-photon, and hence alter this signal strength from the SM prediction. The signal strength is calculated by

$$\mu^{\gamma\gamma} \simeq \frac{\sigma(gg \to h \to \gamma\gamma)}{\sigma(gg \to h \to \gamma\gamma)_{\rm SM}} = R_{gg} \times R_{\gamma\gamma}. \tag{47}$$

We show our results in Fig. 8 for the color-triplet **6**-plet (left panel) and **10**-plet fermions. The left panel shows the results for the **6**-plet case presented in the right panel of Fig. 3. The solid and dashed lines correspond to the same types of lines in the left panel of Fig. 3. The results for the **10**-plet case, which correspond to the dotted and dash-dotted lines in Fig. 5, are depicted in the right panel. As in Fig. 6, the dotted line represents the case with the periodic boundary condition, while the dash-dotted line corresponds to the case with the half-periodic boundary condition.

Employing the constraint $0.96 \leq \mu^{\gamma\gamma} \leq 1.33$ from the ATLAS and CMS combined analysis [4], we can find a lower bound on m_0 from Fig. 8. No lower bound can be obtained from the results on the left panel. For the **6**-plet fermions, we may apply the lower bound presented in Table 1. When we assign $Q = 4/3$ to the **6**-plet fermions, the lightest mode has the color triplet with an electric charge $2/3$, so that it can generally mix with the SM top quark. Through this mixing, once produced dominantly through the gluon fusion process at the LHC, it can decay into the W-boson/Z-boson/Higgs boson and top/bottom quark through the charged/neutral current. The current search

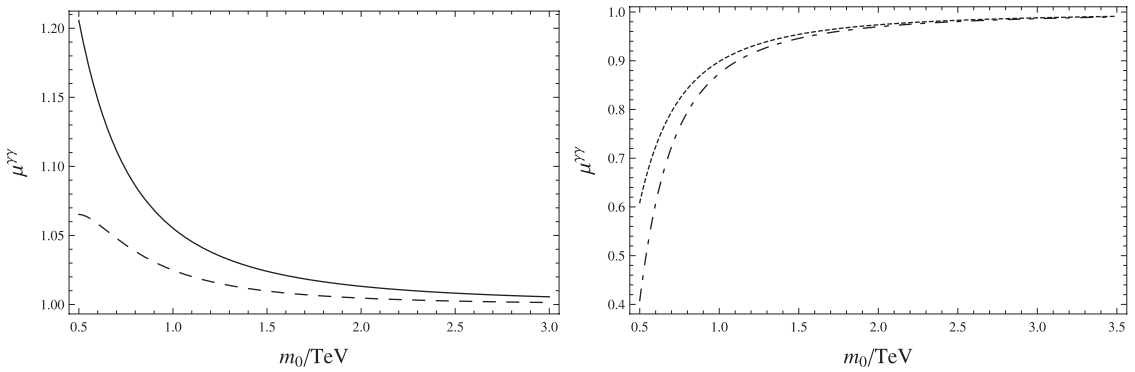

Fig. 8. The signal strength as a function of the lightest bulk fermion mass m_0. The left panel shows the results for the **6**-plet case corresponding to the right panel of Fig. 3. The results for the **10**-plet case, corresponding to the dotted and dash-dotted lines in Fig. 5, are depicted in the right panel. Here we have considered the periodic boundary condition for the dotted line in Fig. 5, and the half-periodic boundary condition for the dash-dotted line in Fig. 5. The dotted and dash-dotted lines represent the results for the periodic and half-periodic **10**-plet fermions, respectively.

Table 3. The lower bound on the lightest bulk colored fermion masses and the compactification scales from the ATLAS and CMS combined analysis, $0.96 \leq \mu^{\gamma\gamma} \leq 1.33$. We have obtained the lower bound only for the **10**-plet bulk fermions.

	BC	$N_f^{(\mathrm{HP})}$	Q	m_0 (TeV)	M_{KK} (TeV)
10-plet	P	1	5/3	1.61	2.13
10-plet	HP	1	5/3	1.74	2.01

for such a vector-like color-triplet particle at the LHC has set lower mass limits between 720 and 920 GeV at 95% confidence level [46], which are more severe than those listed in Table 1. The lower bounds on m_0 can be read off from the right panel in Fig. 8 and are summarized in Table 3. Comparing Tables 1 and 3, we see that the lower mass bounds from $\mu^{\gamma\gamma}$ for the **10**-plet are more severe than those from R_{gg} and the direct search at the LHC.

4. Conclusions

Since the discovery of the SM Higgs boson at the LHC, the properties of the Higgs boson have been investigated towards experimental confirmation of the origin of mass and electroweak symmetry breaking in the SM. The LHC Run-2 with the upgrade of the collider energy to 13 TeV is in operation and more data is being accumulated. In the near future, the Higgs boson properties such as its mass and decay rates to a variety of modes will be more accurately measured, by which the Higgs sector in the SM may be precisely confirmed or some deviation from the SM framework may be revealed.

The gauge hierarchy problem is one of the most serious problems of the SM, and new physics models have been proposed towards a solution to the problem. Such new physics models include new particles whose couplings to the SM Higgs doublet influence the Higgs boson properties. For example, in the minimal supersymmetric standard model, there is a correlation between the Higgs boson mass and the mass of sparticles, in particular, scalar top quarks.

In this paper, we have considered the gauge-Higgs unification scenario in 5D flat space-time, where the SM Higgs doublet is embedded in the fifth spacial component of the gauge field in

five dimensions. Thanks to the gauge symmetry, the quadratic divergence of the Higgs self-energy is forbidden and, as a result, the gauge hierarchy problem can be solved. The gauge symmetry also forbids the Higgs potential at the tree level, which is generated through quantum corrections with the breaking of the original bulk gauge symmetry down to the SM one. Thus, once the model is defined, the Higgs potential is in principle calculable and the Higgs boson mass can be predicted. However, it is highly non-trivial to propose a concrete and complete GHU model that can provide not only a realistic (effective) Higgs potential but also all realistic SM fermion mass matrices.

In analyzing the Higgs boson properties in the context of the GHU scenario, there is a powerful approach in the low-energy effective theoretical point of view. Independently of details of the GHU models, the Higgs potential must disappear once the bulk gauge symmetry is restored at some high energy, which is identified as the compactification scale through analysis of the effective Higgs potential in a simple GHU model. In low-energy effective theory where all the KK modes are decoupled, this general feature of the GHU scenario yields the so-called gauge-Higgs condition, namely, the Higgs quartic coupling is set to be zero at the compactification scale. Therefore, under the assumption that the electroweak symmetry breaking is correctly achieved, the Higgs boson mass can be calculated by extrapolating the vanishing Higgs quartic coupling at the compactification scale towards low energies.

For a simple GHU model based on the bulk gauge group $SU(3)\times U(1)'$, we have analyzed the RG equations with the gauge-Higgs boundary condition to reproduce the observed Higgs boson pole mass of $m_H = 125.09$ GeV. If we assume only the SM particle contents below the compactification scale, the Higgs boson mass is realized by $M_{KK} \simeq 10^{10}$ GeV. We have introduced bulk fermions with a bulk mass and imposed a periodic or half-periodic boundary condition. For concreteness, we have considered color-singlet/triplet **6** and **10**-plets of SU(3) with a $U(1)'$ charge Q. Once the fermion representation is fixed, we have found a unique relation between the compactification scale and the bulk mass so as to reproduce $m_H = 125.09$ GeV. In the presence of the bulk fermions with the TeV scale mass, we have found $M_{KK} \ll 10^{10}$ GeV, which is desired from the point of view of naturalness.

We have also investigated the effect of bulk fermions on the Higgs boson phenomenology. The bulk fermions contribute to the effective Higgs couplings to the di-gluon and/or di-photon through quantum correction at the one-loop level and, as a result, the Higgs boson production and decay rates at the LHC can be altered from the SM predictions. We have employed the current LHC data, which are consistent with the SM predictions, and derived the lower mass bound on the lightest KK mode fermion. More precise measurements of the Higgs production and decay rates in the future can indirectly test the existence of the bulk fermions.

As pointed out in Ref. [36], the bulk fermions, if their masses lie in the TeV scale, can also be tested directly at the LHC. A bulk fermion multiplet includes many fermions with a variety of electric charges, and the mass splittings among the fermions are predicted after electroweak symmetry breaking. Hence, a heavy fermion, once produced at the LHC, causes cascade decays to lighter mass eigenstates and weak gauge bosons or the Higgs boson, which end up with the lightest KK mode fermion. The lightest KK mode fermion can be a dark matter candidate if it is electrically neutral and stable, or decays to the SM fermions through mixing with them. The existence of a variety of fermion mass eigenstates and their cascade decay at the LHC is a characteristic feature of our GHU model. The search for KK mode fermions at the LHC Run-2 is an interesting topic and we leave it for future work.

Acknowledgements

We would like to thank Satomi Okada for her useful comments on the manuscript. N.O. would like to thank KEK Theory Center for hospitality during his visit. This work is supported in part by a US Department of Energy Grant, No. DE-SC0013680.

Funding

Open Access funding: SCOAP[3].

References

[1] G. Aad et al. [ATLAS Collaboration], Phys. Lett. B **716**, 1 (2012) [arXiv:1207.7214 [hep-ex]] [Search INSPIRE].
[2] S. Chatrchyan et al. [CMS Collaboration], Phys. Lett. B **716**, 30 (2012) [arXiv:1207.7235 [hep-ex]] [Search INSPIRE].
[3] G. Aad et al. [ATLAS and CMS Collaborations], Phys. Rev. Lett. **114**, 191803 (2015) [arXiv:1503.07589 [hep-ex]] [Search INSPIRE].
[4] G. Aad et al. [ATLAS and CMS Collaborations], J. High Energy Phys. **08**, 045 (2016) [arXiv:1606.02266 [hep-ex]] [Search INSPIRE].
[5] D. Buttazzo, G. Degrassi, P. P. Giardino, G. F. Giudice, F. Sala, A. Salvio, and A. Strumia, J. High Energy Phys. **12**, 089 (2013) [arXiv:1307.3536 [hep-ph]] [Search INSPIRE].
[6] ATLAS, CDF, CMS, and D0 Collaborations, arXiv:1403.4427 [hep-ex] [Search INSPIRE].
[7] A. V. Bednyakov, B. A. Kniehl, A. F. Pikelner, and O. L. Veretin, Phys. Rev. Lett. **115**, 201802 (2015) [arXiv:1507.08833 [hep-ph]] [Search INSPIRE].
[8] J. Elias-Miro, J. R. Espinosa, G. F. Giudice, G. Isidori, A. Riotto, and A. Strumia, Phys. Lett. B **709**, 222 (2012) [arXiv:1112.3022 [hep-ph]] [Search INSPIRE].
[9] G. Dvali, arXiv:1107.0956 [hep-th] [Search INSPIRE].
[10] J. Garriga, B. Shlaer, and A. Vilenkin, J. Cosmol. Astropart. Phys. **11**, 035 (2011) [arXiv:1109.3422 [hep-th]] [Search INSPIRE].
[11] M. Dine, P. Draper, and C.-S. Park, Phys. Rev. D **86**, 065033 (2012) [arXiv:1206.5880 [hep-th]] [Search INSPIRE].
[12] M. Fairbairn and R. Hogan, Phys. Rev. Lett. **112**, 201801 (2014) [arXiv:1403.6786 [hep-ph]] [Search INSPIRE].
[13] A. Kobakhidze and A. Spencer-Smith, arXiv:1404.4709 [hep-ph] [Search INSPIRE].
[14] G. Lazarides, Q. Shafi, and C. Wetterich, Nucl. Phys. B **181**, 287 (1981).
[15] R. N. Mohapatra and G. Senjanović, Phys. Rev. D **23**, 165 (1981).
[16] M. Magg and Ch. Wetterich, Phys. Lett. B **94**, 61 (1980).
[17] J. Schechter and J. W. F. Valle, Phys. Rev. D **22**, 2227 (1980).
[18] R. Foot, H. Lew, X.-G. He, and G. C. Joshi, Z. Phys. C **44**, 441 (1989).
[19] I. Gogoladze, N. Okada, and Q. Shafi, Phys. Rev. D **78**, 085005 (2008) [arXiv:0802.3257 [hep-ph]] [Search INSPIRE].
[20] P. S. Bhupal Dev, D. K. Ghosh, N. Okada, and I. Saha, J. High Energy Phys. **03**, 150 (2013); **05**, 049 (2013) [erratum] [arXiv:1301.3453 [hep-ph]] [Search INSPIRE].
[21] I. Gogoladze, N. Okada, and Q. Shafi, Phys. Lett. B **668**, 121 (2008) [arXiv:0805.2129 [hep-ph]] [Search INSPIRE].
[22] B. He, N. Okada, and Q. Shafi, Phys. Lett. B **716**, 197 (2012) [arXiv:1205.4038 [hep-ph]] [Search INSPIRE].
[23] N. S. Manton, Nucl. Phys. B **158**, 141 (1979).
[24] D. B. Fairlie, Phys. Lett. B **82**, 97 (1979).
[25] D. B. Fairlie, J. Phys. G **5**, L55 (1979).
[26] Y. Hosotani, Phys. Lett. B **126**, 309 (1983).
[27] Y. Hosotani, Phys. Lett. B **129**, 193 (1983).
[28] Y. Hosotani, Annals Phys. **190**, 233 (1989).
[29] H. Hatanaka, T. Inami, and C. S. Lim, Mod. Phys. Lett. A **13**, 2601 (1998) [arXiv:hep-th/9805067] [Search INSPIRE].

[30] N. Haba, S. Matsumoto, N. Okada, and T. Yamashita, J. High Energy Phys. **02**, 073 (2006) [arXiv:hep-ph/0511046] [Search INSPIRE].
[31] N. Haba, S. Matsumoto, N. Okada, and T. Yamashita, Prog. Theor. Phys. **120**, 77 (2008) [arXiv:0802.3431 [hep-ph]] [Search INSPIRE].
[32] I. Gogoladze, N. Okada, and Q. Shafi, Phys. Lett. B **655**, 257 (2007) [arXiv:0705.3035 [hep-ph]] [Search INSPIRE].
[33] I. Gogoladze, N. Okada, and Q. Shafi, Phys. Lett. B **659**, 316 (2008) [arXiv:0708.2503 [hep-ph]] [Search INSPIRE].
[34] I. Gogoladze, N. Okada, and Q. Shafi, arXiv:1307.5079 [hep-ph] [Search INSPIRE].
[35] N. Maru and N. Okada, Phys. Rev. D **87**, 095019 (2013) [arXiv:1303.5810 [hep-ph]] [Search INSPIRE].
[36] N. Maru and N. Okada, arXiv:1310.3348 [hep-ph] [Search INSPIRE].
[37] C. A. Scrucca, M. Serone, and L. Silvestrini, Nucl. Phys. B **669**, 128 (2003) [arXiv:hep-ph/0304220] [Search INSPIRE].
[38] G. Cacciapaglia, C. Csáki, and S. C. Park, J. High Energy Phys. **03**, 099 (2006) [arXiv:hep-ph/0510366] [Search INSPIRE].
[39] N. Haba, S. Matsumoto, N. Okada, and T. Yamashita, J. High Energy Phys. **03**, 064 (2010) [arXiv:0910.3741 [hep-ph]] [Search INSPIRE].
[40] M. Regis, M. Serone, and P. Ullio, J. High Energy Phys. **03**, 084 (2007) [arXiv:hep-ph/0612286] [Search INSPIRE].
[41] G. Panico, E. Pontón, J. Santiago, and M. Serone, Phys. Rev. D **77**, 115012 (2008) [arXiv:0801.1645 [hep-ph]] [Search INSPIRE].
[42] M. Carena, A. D. Medina, N. R. Shah, and C. E. M. Wagner, Phys. Rev. D **79**, 096010 (2009) [arXiv:0901.0609 [hep-ph]] [Search INSPIRE].
[43] Y. Hosotani, P. Ko, and M. Tanaka, Phys. Lett. B **680**, 179 (2009) [arXiv:0908.0212 [hep-ph]] [Search INSPIRE].
[44] J. Ellis, M. K. Gaillard, and D. V. Nanopoulos, Nucl. Phys. B **106**, 292 (1976).
[45] N. Maru and N. Okada, Phys. Rev. D **77**, 055010 (2008) [arXiv:0711.2589 [hep-ph]] [Search INSPIRE].
[46] V. Khachatryan et al. [CMS Collaboration], Phys. Rev. D **93**, 012003 (2016) [arXiv:1509.04177 [hep-ex]] [Search INSPIRE].